Available online at www.sciencedirect.com
SCIENCE DIRECT®
Journal of Organometallic Chemistry 690 (2005) 1739–1749
Journal of Organometallic Chemistry
www.elsevier.com/locate/jorganchem

Bridged bis-pyridinylimino dinickel(II) complexes: Syntheses, characterization, ethylene oligomerization and polymerization

Suyun Jie [a], Dongheng Zhang [a], Tianzhu Zhang [a], Wen-Hua Sun [a,*], Jiutong Chen [b], Qing Ren [b], Dongbing Liu [c], Gang Zheng [c], Wei Chen [c,*]

[a] Key Laboratory of Engineering Plastics, Institute of Chemistry, Chinese Academy of Sciences, Beijing 100080, China
[b] State Key Laboratory of Structural Chemistry, Fujian Institute of Research on the Structure of Matter, Chinese Academy of Sciences, Fuzhou 350002, China
[c] Polyolefin National Engineering and Research Center, Beijing Research Institute of Chemical Industry, China Petroleum & Chemical Corporation, Beijing 100013, China

Received 29 November 2004; accepted 20 January 2005
Available online 25 February 2005

Abstract

A series of bridged bis(pyridinylimino) ligands were efficiently synthesized through the condensation reaction of 4,4′-methylene-bis(2,6-disubstituted aniline) with 2-pyridinecarboxaldehyde or 2-benzoylpyridine. They reacted with (DME)$NiBr_2$ to form dinuclear Ni(II) complexes. All resultant compounds were characterized by elemental analysis, IR spectra as well as the single-crystal X-ray diffraction to confirm the structures of ligands and complexes. Activated with methylaluminoxane (MAO), these nickel complexes showed considerably good activities for ethylene oligomerization and polymerization. Their catalytic activities and the properties of PEs obtained were depended on the arched environment of ligand and reaction conditions.

Keywords: Bis(pyridinylimino) ligand; Nickel complexes; Ethylene oligomerization; Polymerization

1. Introduction

In the past decade, homogeneous "non-metallocene" catalytic systems for the ethylene polymerization have drawn much attention, particularly late-transition metal derivatives [1]. The nickel complex was evidentially proved as good catalyst for ethylene oligomerization in SHOP process [2]. In 1995, the pioneering work by Brookhart's group on α-diimino nickel complexes for high molecular weight polyethylene broke out the silence of late-transition metal catalysts for polyolefins [3], and resulted in the remarkable increase of academic publications and patents about polyolefins obtained with Group VIII metal complexes as catalysts [1]. The various Schiff-base ligands such as N̂N [3,4] and N̂N̂N [5] ligands have been extensively studied based on their easy preparation and the promising catalytic properties of their late-transition metal complexes. Involved in the exploring alternative nickel complexes as catalysts for ethylene activation, the bidentate and tridentate pyridinylimino derivatives are also generally considered in our group [6]. Pyridinylimino nickel complexes were observed as the centrosymmetric dimers with two bridging bromine atoms around each five-coordination nickel center [4] or the monomers with one acetonitrile

* Corresponding authors. Tel.: +86 10 62557955; fax: +86 10 62618239.
E-mail addresses: whsun@iccas.ac.cn (W.-H. Sun), chenwei@brici.ac.cn (W. Chen).

0022-328X/$ - see front matter © 2005 Elsevier B.V. All rights reserved.
doi:10.1016/j.jorganchem.2005.01.029

molecule around five-coordination nickel center [7] in different solvents, all these nickel complexes showed good activities for ethylene polymerization. Investigating the scope of such nickel complexes and their catalytic activities, it would be interesting to synthesize the bridged bis(pyridinylimino) ligands and their nickel complexes. The 4,4′-methylene-bis(2,6-disubstituted aniline) were employed in the reaction with 2-pyridinecarboxaldehyde or 2-benzoylpyridine to form the bridged bis(pyridinylimino) ligands (**L1–L4**) and (**L5–L8**) [8], respectively. The bridged bis(pyridinylimino) ligands reacted with (DME)$NiBr_2$ to form their corresponding dinuclear nickel complexes (**C1–C8**). In the presence of methylaluminoxane (MAO), these nickel complexes showed considerably good activities for ethylene oligomerization and polymerization. Herein, the synthesis and characterization of ligands and nickel complexes were reported, and the nickel complexes for ethylene oligomerization and polymerization were carefully examined with various catalytic conditions.

2. Results and discussion

2.1. Synthesis and characterization of the ligands and complexes

All the bridged bis(pyridinylimino) ligands were synthesized in the high yields by the condensation reaction. The ligands **L1–L4** were prepared by simply mixing 4,4′-methylene-bis(2,6-disubstituted aniline) and 2-pyridinecarboxaldehyde in ethanol with the catalytic amount of p-toluene sulfonic acid. On stirring for one day at room temperature, the ligands precipitated from the reaction mixture were isolated by filtration and purified by re-crystallization from their ethanol solutions (see Scheme 1). All the four ligands were characterized by elemental analysis, IR and ^1H NMR spectra. In the synthesis of the bulky **L5–L8**, it was necessary to remove the water formed in the reaction by using tetraethyl orthosilicate according to our previous work [8].

The bridged bis(pyridinylimino) ligands easily reacted with 2 equiv. of dibromo(1,2-dimethoxyethane)nickel (II) [(DME)$NiBr_2$] in CH_2Cl_2 to form the corresponding bridged bis(pyridinylimino) dinuclear nickel complexes (see Scheme 2). The complexes **C1–C8** were characterized with elemental analysis and IR spectra. In the IR spectra of ligands **L1–L4** and **L5–L8**, strong and sharp peaks observed in the ranges of 1638–1643 and 1627–1632 cm^{-1}, respectively, were ascribed to the stretching vibration of C=N, while the IR absorption bands of C=N appeared in the ranges of 1631–1632 and 1590–1591 cm^{-1} for their corresponding nickel complexes **C1–C4** and **C5–C8**. The elemental analysis confirmed the components of ligands and nickel complexes. However, some elemental data of nickel complexes showed incorporation of solvent or water molecules due to the samples prepared by re-crystallization. The real structures of the ligands and nickel complexes were confirmed by the single-crystal X-ray diffraction analysis.

2.2. Crystal structures

Single crystals suitable for the X-ray diffraction analysis were obtained by crystallization from the hexane solution of ligand **L4**, the acetonitrile solution of complex **C1** and slow diffusion of diethyl ether to the CH_3OH–DMF solution of complex **C7**, respectively.

The molecular structure of ligand **L4** is showed in Fig. 1 and the selected bond lengths and angles are listed in Table 1. The molecule is composed of two equivalent parts connected by atom C(7) with the bond angle C(5A)–C(7)–C(5) 114.3(4)°. The distance between N(1) and C(12) (1.249(5) Å) is corresponding to the typical bond length of C=N [9]. The two phenyl ring planes, connected through C(7), are almost orthorhombic (the dihedral angle between the two rings is 87.9°).

The molecular structure of complex **C1** is shown in Fig. 2 and the selected bond lengths and angles are listed in Table 2. In complex **C1**, one ligand coordinates with two metal nickel(II) cations. The molecule is composed of two similar parts connected by C(15) and the C(10)–C(15)–C(16) bond angle 113.8(19)°. The dihedral angle between the two aromatic rings connected by C(15) is 78.3°. In the molecule, one nickel (Ni2) is five-coordinated with one acetonitrile molecule on the axial coordination site and the other nickel (Ni1) is six-coordinated with one acetonitrile molecule and one H_2O molecule. Comparing the bond lengths of N–Ni bonds of two nickel atoms, Ni(1)–N(1) 2.123(14) Å to Ni(2)–

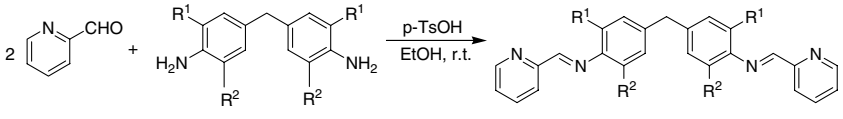

L1: R^1=Me; R^2=Me **L3**: R^1=i-Pr; R^2=i-Pr

L2: R^1=Et; R^2=Et **L4**: R^1=i-Pr; R^2=Me

Scheme 1. The synthesis of ligands **L1–L4**.

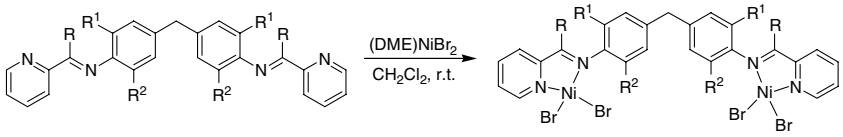

C1: R=H; R^1=Me; R^2=Me **C5**: R=Ph; R^1=Me; R^2=Me

C2: R=H; R^1=Et; R^2=Et **C6**: R=Ph; R^1=Et; R^2=Et

C3: R=H; R^1=i-Pr; R^2=i-Pr **C7**: R=Ph; R^1=i-Pr; R^2=i-Pr

C4: R=H; R^1=i-Pr; R^2=Me **C8**: R=Ph; R^1=i-Pr; R^2=Me

Scheme 2. The synthesis of nickel(II) complexes **C1**–**C8**.

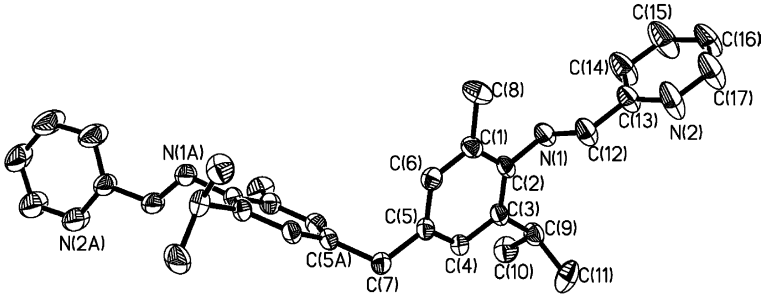

Fig. 1. Crystal structure of **L4**. Displacement ellipsoids are drawn at the 30% probability level. Hydrogen atoms are omitted for clarity.

Table 1
Selected bond lengths (Å) and angles (°) for **L4**

Bond lengths			
N(1)–C(12)	1.249(5)	N(2)–C(13)	1.325(5)
N(1)–C(2)	1.436(4)	N(2)–C(17)	1.338(6)
Bond angles			
C(12)–N(1)–C(2)	118.2(3)	C(13)–N(2)–C(17)	117.7(4)
C(3)–C(2)–N(1)	120.2(3)	C(1)–C(2)–N(1)	118.5(3)
N(1)–C(12)–C(13)	123.5(4)	N(2)–C(13)–C(12)	115.4(4)
N(2)–C(13)–C(14)	121.9(4)	N(2)–C(17)–C(16)	124.4(5)
C(5A)–C(7)–C(5)	114.3(4)		

Symmetry transformations used to generate equivalent atoms: #1 $-x+1, y, -z+1/2$.

N(4) 2.070(16) Å and Ni(1)–N(5) 2.10(2) Å to Ni(2)–N(6) 2.050(16) Å, they are relatively longer for nitrogen atoms bonding with Ni1 due to the coordinated water molecule. However, Ni(1)–N(2) 2.143(17) Å to Ni(2)–N(3) 2.114(17) Å, their bond lengths are the approximately same for the nitrogen atoms of imino groups to two nickel atoms, and there are slight effects on N=C bonds, N(2)–C(6) 1.29(2) Å to N(3)–C(24) 1.21(2) Å. In the structure, the geometry around Ni(2) is slightly distorted trigonal bipyramidal with the equatorial angles ranging from 109.8(4)° to 129.95(14)° and the trans-axial angle of the N(6)–Ni(2)–N(4) is 166.8(7)°, while

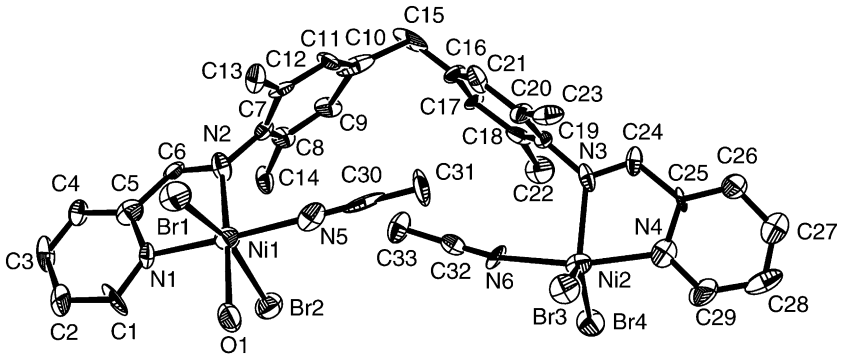

Fig. 2. Molecular structure of **C1**. Displacement ellipsoids are drawn at the 30% probability level. Hydrogen atoms are omitted for clarity.

Table 2
Selected bond lengths (Å) and angles (°) for **C1**

Bond lengths			
Br(1)–Ni(1)	2.592(4)	Ni(2)–N(3)	2.114(17)
Br(2)–Ni(1)	2.620(3)	N(1)–C(1)	1.31(3)
Br(3)–Ni(2)	2.410(3)	N(1)–C(5)	1.34(2)
Br(4)–Ni(2)	2.436(3)	N(2)–C(6)	1.29(2)
Ni(1)–N(5)	2.10(2)	N(2)–C(7)	1.42(2)
Ni(1)–O(1)	2.118(15)	N(3)–C(24)	1.21(2)
Ni(1)–N(1)	2.123(14)	N(3)–C(19)	1.41(2)
Ni(1)–N(2)	2.143(17)	N(4)–C(29)	1.33(3)
Ni(2)–N(6)	2.050(16)	N(4)–C(25)	1.36(2)
Ni(2)–N(4)	2.070(16)	N(6)–C(32)	1.107(19)
Bond angles			
N(5)–Ni(1)–O(1)	91.4(6)	N(2)–Ni(1)–Br(2)	95.6(4)
N(5)–Ni(1)–N(1)	172.3(7)	Br(1)–Ni(1)–Br(2)	163.18(14)
O(1)–Ni(1)–N(1)	94.6(6)	N(6)–Ni(2)–N(4)	166.8(7)
N(5)–Ni(1)–N(2)	92.7(7)	N(6)–Ni(2)–N(3)	89.5(6)
O(1)–Ni(1)–N(2)	174.0(6)	N(4)–Ni(2)–N(3)	77.8(7)
N(1)–Ni(1)–N(2)	81.1(6)	N(6)–Ni(2)–Br(3)	93.7(4)
N(5)–Ni(1)–Br(1)	95.2(5)	N(4)–Ni(2)–Br(3)	94.1(5)
O(1)–Ni(1)–Br(1)	83.7(4)	N(3)–Ni(2)–Br(3)	109.8(4)
N(1)–Ni(1)–Br(1)	90.3(4)	N(6)–Ni(2)–Br(4)	91.2(4)
N(2)–Ni(1)–Br(1)	100.3(4)	N(4)–Ni(2)–Br(4)	91.9(4)
N(5)–Ni(1)–Br(2)	89.4(5)	N(3)–Ni(2)–Br(4)	120.0(4)
O(1)–Ni(1)–Br(2)	80.0(4)	Br(3)–Ni(2)–Br(4)	129.95(14)
N(1)–Ni(1)–Br(2)	86.7(4)	C(16)–C(15)–C(10)	113.8(19)

Table 3
Selected bond lengths (Å) and angles (°) for **C7**

Bond lengths			
Ni–O	2.026(4)	O–C(8)	1.269(7)
Ni–N(1)	2.033(5)	N(1)–C(1)	1.352(7)
Ni–N(2)	2.076(4)	N(1)–C(5)	1.358(7)
Ni–Br(2)	2.4323(16)	N(2)–C(6)	1.310(7)
Ni–Br(1)	2.4538(17)	N(2)–C(21)	1.425(6)
Bond angles			
O–Ni–N(1)	168.59(17)	Br(2)–Ni–Br(1)	122.01(6)
O–Ni–N(2)	90.11(16)	C(1)–N(1)–Ni	125.4(4)
N(1)–Ni–N(2)	78.60(17)	C(5)–N(1)–Ni	116.7(3)
O–Ni–Br(2)	94.83(12)	C(6)–N(2)–C(21)	121.4(4)
N(1)–Ni–Br(2)	90.66(13)	C(6)–N(2)–Ni	114.9(3)
N(2)–Ni–Br(2)	126.52(11)	C(21)–N(2)–Ni	122.1(3)
O–Ni–Br(1)	92.90(12)	N(2)–C(6)–C(11)	125.7(4)
N(1)–Ni–Br(1)	92.66(13)	C(22)–C(21)–N(2)	121.0(4)
N(2)–Ni–Br(1)	110.81(11)	C(24A)–C(7)–C(24)	110.2(6)

Symmetry transformations used to generate equivalent atoms: #1 $-x + 1/2, -y + 1/2, z$.

the geometry around Ni(1) is slightly distorted octahedron.

The molecular structure of complex **C7** is shown in Fig. 3 and the selected bond lengths and angles are listed in Table 3. It can be seen from Fig. 3 that the complex **C7** is composed of the two equivalent parts, in which two phenyl ring planes are connected by atom C(7) with a dihedral angle of 81.7°, and the bond angle C(24A)–C(7)–C(24) is 110.2(6)°. In this molecule, one ligand also coordinates with two nickel(II) cations. Each nickel(II) cation is five-coordinated with one DMF molecule. The X-ray structure shows that the geometry around nickel(II) is slightly distorted trigonal bipyramidal with one DMF molecule on the axial coordination site, in which Br1, Br2 and N2 compose an equatorial plane along with two atoms of N(1) and O occupying the two axial coordination sites, respectively. The nickel is slightly deviated from the triangular plane by −0.0809 Å.

It should be addressed about the previous works of using bridged bis(pyridinylimino) ligands that the nickel analogues reported by Hannon showed a pseudo-octahedral geometry due to three ligands coordinating with two nickel cations [10]. In addition, their silver analogues were also investigated [8,11]. The variation of their coordination was attributed to the bulk of ligands and it is necessary of the steric effects on enforcing the catalytic activity of the nickel complexes [3]. In our concern, the bridged substituted bis(pyridinylimino) ligands were needed, and their preparations were relatively difficult and lower yield of the 4,4′-methylene-bis(2,6-disubstituted aniline) than 4,4′-methylene-di-aniline. Therefore the reagents removing the resultant water are necessary in the reaction with 2-benzoylpyridine for the desired bulky bridged bis(pyridinylimino) ligands [8].

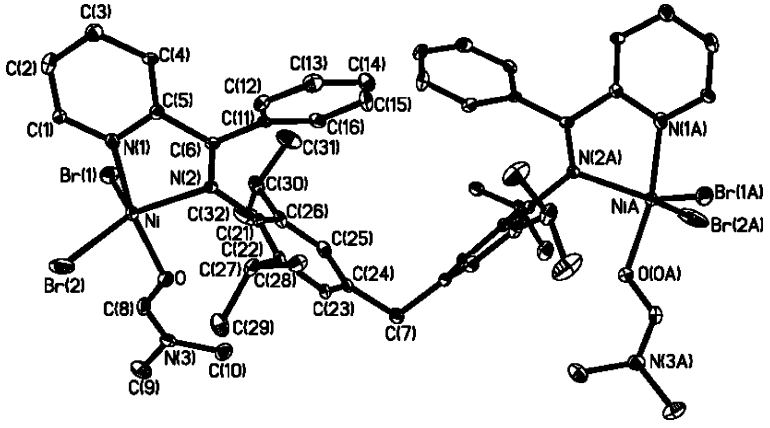

Fig. 3. Molecular structure of **C7**. Displacement ellipsoids are drawn at the 30% probability level. Hydrogen atoms are omitted for clarity.

2.3. Ethylene oligomerization and polymerization

The catalyst precursor **C1**–**C8** could be activated for ethylene oligomerization and polymerization with methylaluminoxane (MAO). The results with one atmosphere of ethylene were summarized in Table 4. The catalytic system of **C2** was typically investigated through varying reaction conditions, such as the molar ratio of cocatalyst (MAO) to nickel complex (Al/Ni), reaction temperature, reaction period and the pressure of ethylene, for the optimum.

2.3.1. Effects of reaction temperature and Al/Ni molar ratio on catalyst activity

With the fixed Al/Ni molar ratio of 1000:1, the reaction temperature significantly affected on the catalytic activity, and the good polymerization activity was obtained at 0 °C (entry 2, Table 4). Along with elevating reaction temperature in the range of −10 °C to 40 °C, the polymerization activity significantly declined, while the amount of oligomers were increased. Up to 60 °C, only trace of polymer was obtained, in addition, the oligomerization activity was also lowered to 42.8 kg mol^{-1} (Ni) h^{-1} (entry 5, Table 4). Elevating the reaction temperature speeds up combined catalytic reactions of oligomerization and polymerization, however, further increasing reaction temperature results in lower catalytic activities due to the lower solubility of ethylene and deactivation of some active centers [6a].

The variation of Al/Ni molar ratio in catalytic system of **C2** was explored at 0 °C. At the Al/Ni molar ratio of 100:1, only oligomer C_4 was formed with lower activity (entry 8, Table 4). When the Al/Ni molar ratio was further enhanced, the polymerization activity efficiently increased. At the Al/Ni molar ratio of 2000, the catalytic system displayed the higher polymerization activity of 712 kg mol^{-1} (Ni) h^{-1} (entry 13, Table 4).

2.3.2. Lifetime of the active catalytic species

The lifetime of a catalyst is one significant factor in the industrial consideration. The effect of reaction time on catalytic activity was studied using **C2**/MAO system at the Al/Ni molar ratio of 1000:1 and 0 °C. The polymerization activity slightly decreased with the reaction time from 0.5 to 2 h (compare entry 6–7 and 2, Table 4). The active species of **C2** were prolonged somehow during

Table 4
The ethylene activation with complexes **C1**–**C8** at 1 atm[a]

Entry	Complex	Al/Ni	T (°C)[b]	Olig-		Poly-		
				A_o[c]	A_p[c]	T_m[d]	M_w[e]	M_w/M_n[e]
1	**C2**	1000	−10	32.5	48.4	n.d.[f]	n.d.	n.d.
2	**C2**	1000	0	48.4	334	124.3, 110.7[i]	8 204	3.66
3	**C2**	1000	20	72.6	177	Wax	n.d.	n.d.
4	**C2**	1000	40	122	25.4	Wax-oil	n.d.	n.d.
5	**C2**	1000	60	42.8	Trace	–	–	–
6[g]	**C2**	1000	0	16.6	324	123.8, 109.0[i]	n.d.	n.d.
7[h]	**C2**	1000	0	9.9	260	124.6, 109.1[i]	n.d.	n.d.
8	**C2**	100	0	41.3	–	–	–	–
9	**C2**	250	0	45.0	4.2	n.d.	n.d.	n.d.
10	**C2**	500	0	38.9	180	125.2, 116.2[i]	n.d.	n.d.
11	**C2**	750	0	13.3	290	124.1, 111.1[i]	n.d.	n.d.
12	**C2**	1500	0	22.1	372	122.6, 105.4[i]	n.d.	n.d.
13	**C2**	2000	0	39.1	712	124.6, 96.4[i]	n.d.	n.d.
14	**C1**	1000	0	13.6	256	124.5, 113.6[i]	7 864	5.28
15	**C3**	1000	0	9.4	638	122.0, 92.2[i]	3 648	3.42
16	**C4**	1000	0	40.2	280	124.4, 108.2[i]	7 381	5.64
17	**C3**	2000	0	108	792	Wax	1 621	2.04
18	**C5**	1000	0	56.0	73.8	Wax	n.d.	n.d.
19	**C6**	1000	0	49.9	2.60	Wax	n.d.	n.d.
20	**C7**	1000	0	60.3	25.2	Wax	n.d.	n.d.
21	**C8**	1000	0	72.0	12.8	Wax	n.d.	n.d.

[a] Reaction conditions: cat: 2.5 μmol; solvent: toluene (30 ml); reaction time: 0.5 h; ethylene pressure: 1 atm.
[b] Reaction temperature.
[c] Activity: in units of kg mol^{-1} (Ni) h^{-1}.
[d] T_m values were determined by DSC with the second heat curves.
[e] M_w and M_w/M_n values were determined by GPC.
[f] Not determined.
[g] Reaction time: 1 h.
[h] Reaction time: 2 h.
[i] Broad melting peak.

the catalytic reaction; however, it was often reported for nickel catalytic species to be deactivated as time going.

2.3.3. Effects of the ligand environment on the catalytic performance

To compare the catalytic results of the analogues as **C1**, **C3** and **C4** at the Al/Ni (1000:1) and 0 °C, **C3** containing the ligand with isopropyl substituents performed the highest polymerization activity (entry 16, Table 4). According to the better polymerization activity of **C2** (entry 13, Table 4) with the Al/Ni (2000:1) at 0 °C, as expected, the polymerization activity of **C3** was improved to 792 kg mol^{-1} (Ni) h^{-1} (entry 17, Table 4). Based on those data, the catalytic activity of the nickel complex is greatly affected by the arched environment of corresponding ligand, and the bulkier substituents, the higher catalytic activity [3].

In addition, to verify the role of the R substituent in the imino-C of the ligands on the catalytic performances, the complexes **C5**–**C8** bearing phenyl on carbon were also studied for ethylene oligomerization and polymerization. Under the same reaction conditions, the complexes **C5**–**C8** displayed the lower polymerization activities and the PEs obtained were wax-like (entry 18–21, Table 4). Though the bulkier group is recognized to increase the catalytic activity of late-transition metal complexes, the conjugated system with phenyl substituent decrease the net charge of the active metal center and reduced its activity as the final result [12].

2.3.4. Effects of ethylene pressure on the catalyst performance

The catalytic reaction was carried out at 10 atm of ethylene pressure and all nickel catalysts showed much better catalytic activity (see Table 5). In the system of **C3**/MAO, the polymerization activity was obtained as high as 2830 kg mol^{-1} (Ni) h^{-1}, and the resultant polyethylene absolutely predominated (entry 3, Table 5). For the complexes **C5**–**C8**/MAO, it was very clear that the ethylene pressure largely affected the catalytic performance (entry 5–8, Table 5). At 10 atm of ethylene pressure, the PEs obtained became powder and the complex **C8** displayed higher polymerization activity (entry 8, Table 5). When the complex **C7** was used, however, lower polymerization activity was observed (entry 7, Table 5). Catalyst **C7** bearing the bulkier isopropyl substituents in the *orthro*-positions of imino N-aryl ring probably limited the insertion ability of ethylene and ethylene cannot easily contact with the cationic active centers in the catalytic system, so the polymerization activity decreased.

As a matter of fact, it is common for the late-transition metal catalytic system to carry out catalytic reaction of ethylene oligomerization and polymerization at the same time. With different views, major products of polyethylene or oligomers have been focused in most publications. In the dinuclear nickel complexes discussed herein, some catalytic systems gave good selectivity for ethylene polymerization with very low proportion of oligomers.

2.3.5. Characterization of polyethylene

The obtained PE samples showed intense bands at about 2920 cm^{-1} ($\nu_{as}CH_2$) and 2851 cm^{-1} (ν_sCH_2). Moreover, two single peaks were present around 1469 and 721 cm^{-1}, respectively, assigned to scissoring and rocking vibrations in the solid state of sequential methylene groups. And a weak peak was found in 1374–1376 cm^{-1} due to the branched methyl symmetrical deformation vibration [13,14]. There were additional bands in characteristic presence of the double bond: a weak peak at 1642–1648 cm^{-1} attributed to stretching vibration absorption band of C=C and similar characteristic peaks of polyethylene obtained by its monomer nickel catalysts [4b].

Table 5
The ethylene activation with complexes **C1**–**C8** at 10 atm[a]

Entry	Complex	Al/Ni	Olig-		Poly-		
			A_o[b]	A_p[b]	T_m[c]	M_w[d]	M_w/M_n[d]
1	**C1**	894	85.2	2135	127.0, 121.6[e]	55 984	18.09
2	**C2**	927	328	874	125.5, 119.4[e]	15 405	9.49
3	**C3**	1000	55.1	2830	124.8, 116.7[e]	7 261	3.43
4	**C4**	927	153	1808	125.5, 118.3[e]	13 612	6.60
5	**C5**	1000	127	954	135.4, 128.3	271 625	45.79
6	**C6**	1000	56.7	1104	124.9, 105.6[e]	14 045	4.58
7	**C7**	1000	93.6	916	85.3[e]	4 531	2.20
8	**C8**	1000	57.2	2454	126.1, 104.8[e]	15 023	4.89

[a] Reaction conditions: cat: 10 μmol; solvent: toluene (1000 ml); the Al/Ni molar ratio: 1000; reaction temperature: 20 °C; reaction time: 1 h; ethylene pressure: 10 atm.
[b] Activity: in units of kg mol^{-1} (Ni) h^{-1}.
[c] T_m values were determined by DSC with the second heat curves.
[d] M_w and M_w/M_n values were determined by GPC.
[e] Broad melting peak.

The melting points (T_m) of resultant PEs were determined by differential scanning calorimetry analysis (DSC). The melting points were varied with the different catalysts and various catalytic conditions in Tables 4 and 5. Examining the data of PEs by using complex **C2** at 1 atm of ethylene and 0 °C, the variation of the Al/Ni molar ratio gave slightly different melting points with two peaks. However, there was a great effect of reaction temperature. At either 1 or 10 atm of ethylene pressure, DSC curves gave two melting peaks. The results suggested that the interaction between two metals possibly created more than one kind of active species during the polymerization.

The molecular weights (M_w) and molecular weight distributions (M_w/M_n) of the obtained PEs were measured by GPC analysis. The relatively wide molecular weight distributions were different from those of PEs obtained using pyridinylimino nickel(II) complexes reported by Laine's group [4c] (see Figs. 4–6). In the catalytic system of **C3**/MAO, when the Al/Ni molar ratio was changed from 1000:1 to 2000:1, both M_w and M_w/M_n became lower (compare entry 15 with 17, Table 4). Higher Al/Ni molar ratio increased the chain transfer reaction to MAO and resulted in lower polymer molecular weight. The narrow molecular distribution could be reasoned as a good ratio of cocatalyst to activate the nickel catalyst and produce the catalytic centers. The effect of ethylene pressure was very clear that the M_w significantly increased and M_w/M_n became broader when the pressure enhanced from 1 to 10 atm (compare Table 4 with 5). For complex **C5**, the highest molecular weight and broadest molecular weight distribution were achieved and as shown by the GPC traces in Fig. 6, the PE sample obtained displayed bimodal molecular weight distribution.

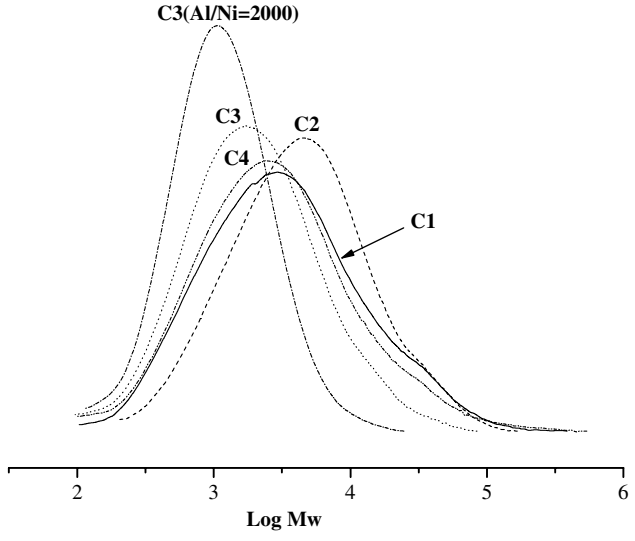

Fig. 4. GPC traces of PE samples obtained by entries 2 and 14–17 in Table 4.

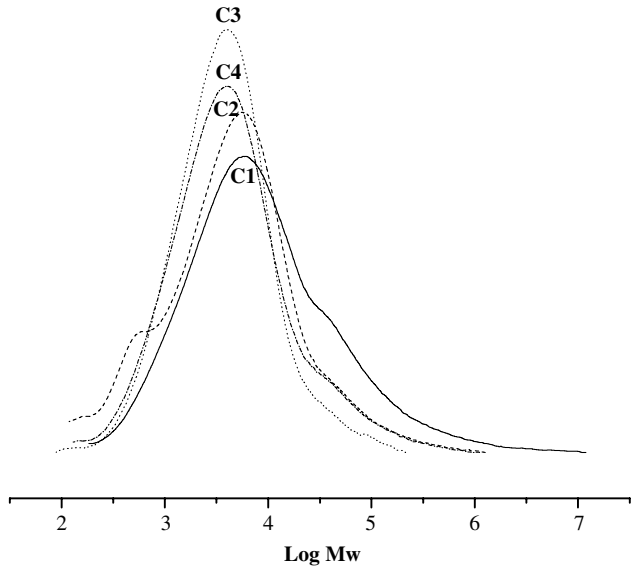

Fig. 5. GPC traces of PE samples obtained by entries 1–4 in Table 5.

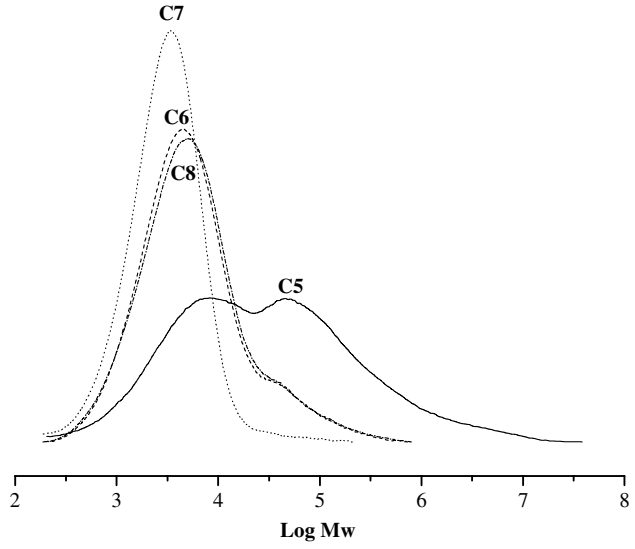

Fig. 6. GPC traces of PE samples obtained by entries 5–8 in Table 5.

The ^1H, ^{13}C NMR spectra were recorded with the PE sample dissolved in *o*-dichlorobenzene-d_4 (see Fig. 7). The ^{13}C NMR spectra of the PE obtained by complex **C3** at 10 atm of ethylene pressure (entry 3, Table 5) indicated that the branched polyethylene with main butyl branch formed and the extent of branching was counted equal to 5 branches per 1000 carbon atoms according to the calculation method reported [15]. The single peaks at δ 114.64 and 139.58 ppm showed the property of vinyl-unsaturated chain end. The assignments were determined according to the literatures [15,16] and the nomenclature of Usami and Takayama [17] for isolated branches was used.

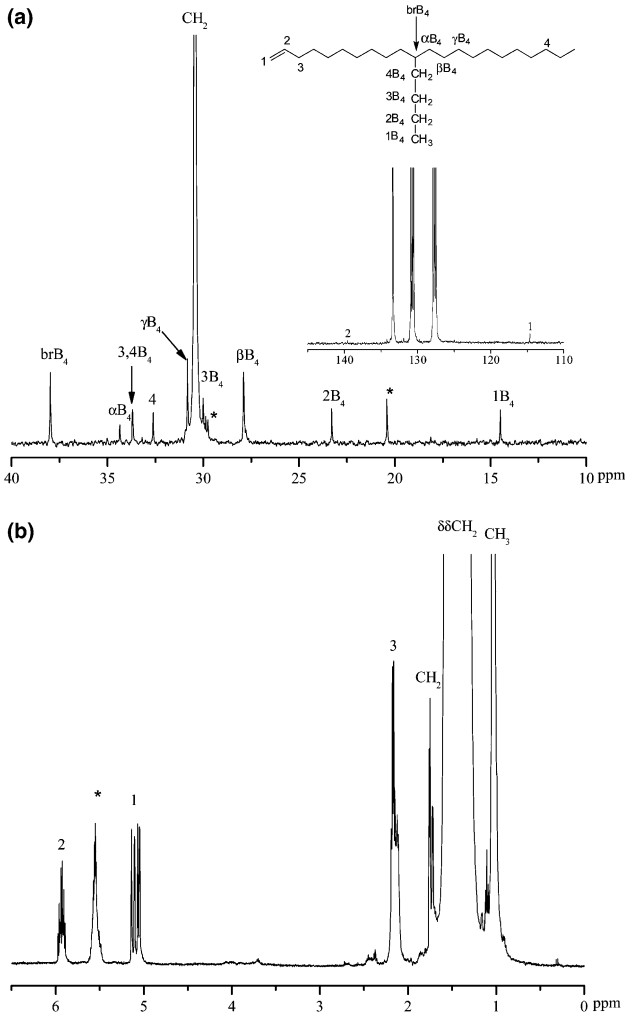

Fig. 7. NMR spectra of polyethylene obtained by entry 3 in Table 5. (a) ^{13}C NMR; (b) ^{1}H NMR. Peaks marked with an asterisk were not assigned.

3. Experimental

3.1. General

All manipulations involving air- and/or moisture-sensitive compounds were carried out under an atmosphere of nitrogen using standard Schlenk techniques. Solvents were refluxed over the appropriate drying reagents and distilled under nitrogen prior to use. IR spectra were recorded on a Perkin–Elmer System FT-IR 2000 spectrometer using KBr disc. ^{1}H NMR spectra were recorded on a Bruker DMX 300 MHz instrument at ambient temperature using TMS as the internal standard. Mass spectra were measured on a Bruker BIFLEX™ III MALDI-TOF. Melting points were measured with a digital electrothermal apparatus without calibration. Elemental analyses were carried out using Flash EA1112 microanalyzer. GC analyses were performed with a Carlo Erba Strumentazione gas chromatograph equipped with a flame ionization detector and a 30 m (0.25 mm i.d., 0.25 μm film thickness) DM-1 silica capillary column. ^{1}H and ^{13}C NMR spectra of the PE sample were recorded on a Bruker DMX 400 MHz instrument at 135 °C in *o*-dichlorobenzene-d_4 using TMS as the internal standard. The molecular weight and the molecular weight distribution of the PEs were determined by a PL-GPC220 instrument at 150 °C with 1,2,4-trichlorobenzene as the eluent. Melting points of the PEs were obtained on a PerkinElmer DSC-7 instrument. The instrument was initially calibrated for the melting point of an indium standard at a heating rate of 10 °C/min. (DME)$NiBr_2$ was purchased from Alfa Aesar. Methylaluminoxane (MAO, 1.4 mol l^{-1} in toluene) was purchased from Albemarle Corp (USA). All other chemicals were obtained from commercial sources unless stated otherwise.

3.2. Preparation of the ligands (*L1–L4*)

The ligands (**L1**–**L4**) were prepared by condensing corresponding 4,4′-methylene-bis(2,6-bissubstituted-aniline) with 2-pyridinecarboxaldehyde in ethanol. Typically, 4,4′-Methylene-*N*,*N*′-(2-pyridinylmethylene)-bis-(2,6-dimethylanil) (**L1**) was synthesized by mixing 4,4′-methylene-bis(2,6-dimethylaniline) (0.631 g, 2.5 mmol) and 2-pyridinecarboxaldehyde (0.614 g, 5.7 mmol) in 10 ml ethanol (95%) along with the catalytic amount of p-toluene sulfonic acid. The reaction mixture was stirred for one day at room temperature, and resulting yellow precipitate was isolated by filtration and re-crystallized from its ethanol solution to give **L1** in 63.3% yield, m.p. 174–176 °C. FT-IR (cm^{-1}): 3435, 2967, 2915, 1643, 1586, 1567, 1479, 1463, 1377, 1202, 1146, 874, 845, 778, 743. ^{1}H NMR (δ, ppm): 8.69 (d, 2H), 8.33 (s, 2H, C*H*=N), 8.27 (d, 2H), 7.82 (t, 2H), 7.39 (m, 2H), 6.93 (s, 4H), 3.84 (s, 2H, CH_2), 2.14 (t, 12H, PhCH_3). Anal. Calc. for $C_{29}H_{28}N_4$: C, 80.52; H, 6.52; N, 12.95. Found: C, 80.63; H, 6.64; N, 12.72%. 4,4′-Methylene-*N*,*N*′-(2-pyridinylmethylene)-bis(2,6-diethyl-anil) (**L2**) was prepared as yellow crystals in 61.0% yield, m.p. 117–119 °C. FT-IR (cm^{-1}): 3054, 2966, 2932, 2872, 1640, 1584, 1569, 1468, 1439, 1199, 1145, 993, 880, 776. ^{1}H NMR (δ, ppm): 8.72 (t, 2H), 8.36 (s, 2H, C*H*=N), 8.28 (d, 2H), 7.85 (t, 2H), 7.41 (m, 2H), 6.97 (s, 4H), 3.95 (s, 2H, CH_2), 2.51 (m, 8H, CH_2Me), 1.13 (t, 12H, CH_3). Anal. Calc. for $C_{33}H_{36}N_4$: C, 81.11; H, 7.43; N, 11.47. Found: C, 80.99; H, 7.45; N, 11.23%. 4,4′-Methylene-*N*,*N*′-(2-pyridinylmethylene)-bis(2,6-diisopropyl-anil) (**L3**) was prepared as yellow crystals in 76.0% yield, m.p. 163–164 °C. FT-IR (cm^{-1}): 3433, 2961, 2929, 2868, 1638, 1585, 1568, 1468, 1439, 1120, 1167, 992, 875, 780. ^{1}H NMR (δ, ppm): 8.73 (d, 2H), 8.32 (s, 2H, C*H*=N), 8.27 (d, 2H), 7.85 (t, 2H), 7.42 (m, 2H), 7.02 (s, 4H), 4.02 (s, 2H, CH_2), 2.96 (m, 2H, C*H*Me$_2$), 1.15 (d, 24H, *i*-Pr-*H*). Anal. Calc. for $C_{37}H_{44}N_4$: C, 81.57; H, 8.14;

N, 10.28. Found: C, 81.28; H, 8.17; N, 10.15%. 4,4′-Methylene-*N*,*N*′-(2-pyridinylmethylene)-bis(2-isopropy-6-methyl-anil) (**L4**) was prepared as yellow crystals in 58.7% yield, m.p. 152–154 °C. FT-IR (cm^{-1}): 3433, 2959, 2927, 2869, 1639, 1586, 1569, 1473, 1438, 1201, 1170, 1133, 887, 865, 774. ^1H NMR (δ, ppm): 8.72 (d, 2H), 8.34 (s, 2H, C*H*=N), 8.28 (d, 2H), 7.85 (t, 2H), 7.41 (m, 2H), 7.04 (s, 2H), 6.92 (s, 2H), 3.93 (s, 2H, CH_2), 3.03 (m, 2H, C*H*Me$_2$), 2.13 (t, 6H, PhCH_3), 1.17 (d, 12H, i-Pr-*H*). Anal. Calc. for $C_{33}H_{36}N_4$: C, 81.11; H, 7.43; N, 11.47. Found: C, 80.73; H, 7.55; N, 11.29%.

3.3. Preparation of the nickel(II) complexes

The nickel complex (**C1**) was obtained in mixing ligand **L1** (0.35 g, 0.8 mmol) and (DME)$NiBr_2$ (0.50 g, 1.6 mmol) in 20 ml dichloromethane using the Schlenk technique, and the reaction mixture was stirred for 24 hrs at room temperature. The resulting precipitate was filtered, washed with diethyl ether and dried in vacuum to form **C1** as a yellow powder in 93.5% yield. FT-IR (cm^{-1}): 3353, 2965, 2923, 1632, 1598, 1482, 1447, 1305, 1199, 1145, 1024, 774. Anal. Calc. for $C_{29}H_{28}Br_4N_4Ni_2 \cdot CH_2Cl_2$: C, 37.75; H, 3.17; N, 5.87. Found: C, 38.02; H, 3.67; N, 5.50%. In a similar manner, the complex **C2** to **C8** were prepared from the ligand **L2** and (DME)$NiBr_2$. **C2** is a yellow powder in 98.1% yield. FT-IR (cm^{-1}): 3371, 2965, 1630, 1597, 1459, 1305, 1197, 1142, 1023, 911, 774. Anal. Calc. for $C_{33}H_{36}Br_4N_4Ni_2$: C, 42.82; H, 3.92; N, 6.05. Found: C, 42.61; H, 4.37; N, 5.96%. **C3** is a yellow powder in 88.5% yield. FT-IR (cm^{-1}): 3372, 2965, 2869, 1631, 1598, 1464, 1446, 1363, 1305, 1198, 1163, 1118, 1023, 910, 775. Anal. Calc. for $C_{37}H_{44}Br_4N_4Ni_2$: C, 45.26; H, 4.52; N, 5.71. Found: C, 45.82; H, 4.97; N 5.54%. **C4** is a yellow powder in 90.7% yield. FT-IR (cm^{-1}): 3347, 2965, 2870, 1632, 1599, 1479, 1447, 1306, 1199, 1161, 1131, 1024, 774. Anal. Calc. for $C_{33}H_{36}Br_4N_4Ni_2 \cdot 2H_2O$: C, 41.21; H, 4.19; N, 5.83. Found: C, 41.54; H, 4.34; N, 5.55%. **C5** is a brown powder in 69.0% yield. FT-IR (cm^{-1}): 3371, 2019, 1590, 1475, 1443, 1381, 1329, 1262, 1217, 1176, 1135, 1108, 1026, 985, 852, 800, 752, 704. MALDI-TOF MS Calcd for $C_{41}H_{37}{}^{79}Br_2N_4Ni_2$ [M-2Br]: 859.8. Found: 860.2. Anal. Calc. for $C_{41}H_{36}Br_4N_4Ni_2 \cdot 2Et_2O$: C, 50.26; H, 4.79; N, 4.79. Found: C, 50.26; H, 4.89; N, 5.32%. **C6** is a brown powder in 66.0% yield. FT-IR (cm^{-1}): 3367, 2970, 2936, 2879, 2319, 1989, 1590, 1445, 1378, 1328, 1262, 1176, 1131, 1061, 1026, 984, 940, 882, 853, 801, 751, 703. MALDI-TOF MS Calcd for $C_{45}H_{45}{}^{79}Br_2N_4Ni_2$ [M-2Br]: 915.9. Found: 916.1. Anal. Calc. for $C_{45}H_{44}Br_4N_4Ni_2 \cdot 1.5Et_2O$: C, 51.47; H, 4.96; N, 4.71. Found: C, 51.01; H, 5.51; N, 4.88%. **C7** is a brown powder in 60.0% yield. FT-IR (cm^{-1}): 3377, 2969, 2871, 2318, 1591, 1465, 1444, 1384, 1363, 1328, 1261, 1158, 1111, 1071, 1028, 985, 958, 799, 753, 703. MALDI-TOF MS Calcd for $C_{49}H_{53}{}^{79}Br_2N_4Ni_2$ [M-2Br]: 972.0. Found: 972.4. Anal. Calc. for $C_{49}H_{52}Br_4N_4Ni_2 \cdot Et_2O$: C, 52.64; H, 5.13; N, 4.64. Found: C, 52.76; H, 5.36; N, 4.67%. **C8** is a brown powder in 80.0% yield. FT-IR (cm^{-1}): 3370, 2965, 2928, 2869, 2355, 2589, 1591, 1470, 1443, 1384, 1328, 1262, 1160, 1123, 1082, 1060, 1026, 984, 857, 800, 753, 703. MALDI-TOF MS Calcd for $C_{45}H_{45}{}^{79}Br_2N_4Ni_2$ [M-2Br]: 915.9. Found: 916.2. Anal. Calc. for $C_{45}H_{44}Br_4N_4Ni_2 \cdot 1.5Et_2O$: C, 51.47; H, 4.96; N, 4.71. Found: C, 51.68; H, 5.38; N, 4.64%.

3.4. X-ray crystallography of *L2*, *C1* and *C7*

Data sets were collected with a RIGAKU SMART CCD diffractometer with graphite monochromatic Mo Kα radiation (λ = 0.71073 Å). Cell parameters were obtained by the global refinement of the positions of all collected reflections. Intensities were corrected for Lorentz and polarization effects and empirical absorption. The structures were solved by direct methods, and refined by full-matrix least-square on F^2. Each hydrogen atom was placed in a calculated position, and refined using a riding model. All non-hydrogen atoms were refined anisotropically. Structure solution and refinement were performed using SHELXL-97 package [18]. The crystal data and refinement parameters were summarized in Table 6.

3.5. Ethylene oligomerization and polymerization

Ethylene oligomerization and polymerization at 1 atm of ethylene pressure was carried out as follows: The catalyst precursor (nickel complex) was dissolved with toluene in a Schlenk tube stirred with a magnetic stirrer under ethylene atmosphere (1 atm), and the reaction temperature was controlled by water bath. The reaction was initiated by adding the desired amount of methylaluminoxane (MAO). After the desired period of time, a small amount of the reaction solution was collected with a syringe, terminated by the addition of 5% aqueous hydrogen chloride, and the analysis by gas chromatography (GC) was carried out for determining the distribution of oligomers obtained. The residual solution was quenched with HCl-acidified ethanol (5%), its precipitated polyethylene was collected by filtration, washed with ethanol, dried in vacuum at 60 °C until constant weight, weighed and finally characterized.

Ethylene oligomerization and polymerization at 10 atm of ethylene pressure was carried out in a 2000-ml autoclave stainless steel reactor equipped with a mechanical stirrer and a temperature controller. The desired amount of MAO, 10 ml toluene solution of nickel complex and 1000 ml of toluene were added to the reactor in this order under ethylene atmosphere. When being

Table 6
Crystal data and structure refinement for **L4**, **C1** and **C7**

	L4	**C1**	**C7**
Empirical formula	$C_{33}H_{36}N_4$	$C_{29}H_{28}Br_4N_4Ni_2 \cdot 2CH_3CN \cdot H_2O$	$C_{49}H_{52}Br_4N_4Ni_2 \cdot 2DMF$
Formula weight	488.66	969.74	1280.20
Crystal color	Yellow	Brown	Red
Temperature (K)	293(2)	293(2)	123.15
Wavelength (Å)	0.71073	0.71073	0.7107
Crystal system	Monoclinic	Monoclinic	Orthorhombic
Space group	C 2/c	P 2(1)	F dd2
a (Å)	14.4681(7)	8.1176(16)	34.60(3)
b (Å)	9.5641(4)	13.245(3)	35.76(3)
c (Å)	21.7672(6)	16.774(3)	9.049(7)
α (°)	90	90	90
β (°)	99.846(2)	95.36(3)	90
γ (°)	90	90	90
Volume (Å^3)	2967.7(2)	1795.7(6)	11196(15)
Z	4	2	8
D_{calc} (Mg m^{-3})	1.094	1.794	1.519
μ (mm^{-1})	0.065	5.535	3.572
F(000)	1048	960	5200
Crystal size (mm)	$0.46 \times 0.40 \times 0.36$	$0.20 \times 0.20 \times 0.06$	$0.45 \times 0.18 \times 0.15$
θ range (°)	1.90–25.01	1.22–27.40	2.28–28.28
Limiting indices	$-17 \leqslant h \leqslant 14$, $-7 \leqslant k \leqslant 11$, $-25 \leqslant l \leqslant 23$	$0 \leqslant h \leqslant 10$, $0 \leqslant k \leqslant 17$, $-21 \leqslant l \leqslant 21$	$-38 \leqslant h \leqslant 46$, $-47 \leqslant k \leqslant 47$, $-12 \leqslant l \leqslant 12$
Reflections collected	4543	4217	22907
Unique reflections	2593 [R_{int} = 0.0405]	4217[R_{int} = 0.0000]	6845[R_{int} = 0.0635]
Completeness to θ (%)	98.7 (θ = 25.01)	98.8 (θ = 27.40)	99.8 (θ = 28.28)
Absorption correction	Empirical	Empirical	Empirical
Max./min. transmission	1.0000/0.2770	1.4037/0.3333	1.0000/0.5923
Data/restraints/parameters	2593/0/241	4217/1/415	6845/1/312
Goodness-of-fit on F^2	1.145	0.873	1.005
Final R indices [$I > 2\sigma(I)$]	R_1 = 0.0873, wR_2 = 0.2081	R_1 = 0.0731, wR_2 = 0.1246	R_1 = 0.0432,wR_2 = 0.1250
R indices(all data)	R_1 = 0.1325, wR_2 = 0.2474	R_1 = 0.2001, wR_2 = 0.1557	R_1 = 0.0563, wR_2 = 0.1382
Largest diff peak and hole (e Å^{-3})	0.181 and −0.222	0.629 and −0.514	0.984 and −0.884

to the reaction temperature, ethylene with the desired pressure (10 atm) was introduced to start the reaction. After 1 h, the reaction was stopped. And then a small amount of the reaction solution was collected, terminated by the addition of 5% aqueous hydrogen chloride and then analyzed by gas chromatography (GC) for determining the distribution of oligomers obtained. Then the residual solution was quenched with HCl-acidified ethanol (5%). The precipitated polymer was collected by filtration, washed with ethanol, dried in vacuum at 60 °C until constant weight, weighed and finally characterized.

Acknowledgements

We are grateful to the National Natural Science Foundation of China for financial supports under Grant No. 20473099 and 20272062, National 863 Foundation (2002AA333060). This work was partly carried out in Polymer Chemistry Laboratory, Chinese Academy of Sciences and China-Petro-Chemical Corporation.

Appendix A. Supplementary data

Supplementary data associated with this article can be found, in the online version, at doi:10.1016/j.jorganchem.2005.01.029.

References

[1] (a) S.D. Ittle, L.K. Johnson, M. Brookhart, Chem. Rev. 103 (2000) 1169;
(b) V.C. Gibson, S.K. Spitzmessor, Chem. Rev. 103 (2003) 283;
(c) S. Mecking, Angew. Chem., Int. Ed. Engl. 40 (2001) 534.
[2] W. Keim, F.H. Kowalt, R. Goddard, C. Kriiger, Angew. Chem., Int Ed. Engl. 17 (1978) 466.
[3] L.K. Johnson, C.M. Killian, M. Brookhart, J. Am. Chem. Soc. 117 (1995) 6414.
[4] (a) T.V. Laine, M. Klinga, M. Leskelä, Eur. J. Inorg. Chem. (1999) 959;
(b) T.V. Laine, K. Lappalainen, J. Liimatta, E. Aitola, B. Löfgren, M. Leskelä, Macromol. Rapid Commun. 20 (1999) 487;
(c) T.V. Laine, U. Piironen, K. Lappalainen, M. Klinga, E. Aitola, M. Leskelä, J. Organomet. Chem. 606 (2000) 112.
[5] (a) B.L. Small, M. Brookhart, A.M.A. Bennett, J. Am. Chem. Soc. 120 (1998) 4049;

(b) G.J.P. Britovsek, V.C. Gibson, B.S. Kimberley, D.J. Williams, Chem. Commun. (1998) 849.
[6] (a) W.-H. Sun, Z. Li, H. Hu, B. Wu, H. Yang, N. Zhu, X. Leng, H. Wang, New J. Chem. 26 (2002) 1474;
(b) L. Wang, W.-H. Sun, L. Han, H. Yang, Y. Hu, X. Jin, J. Organomet. Chem. 658 (2002) 62;
(c) X. Tang, Y. Cui, W.-H. Sun, Z. Miao, S. Yan, Polym. Int. 53 (2004) 2155;
(d) C. Shao, W.-H. Sun, Z. Li, Y. Hu, L. Han, Cat. Commun. 3 (2002) 405.
[7] G.J.P. Britovsek, S.P.D. Baugh, C. Redshaw, O. Hoarau, V.C. Gibson, D.F. Wass, A.J.P. White, D.J. Williams, Inorganica Chimica Acta 345 (2003) 279.
[8] W.-H. Sun, T. Zhang, L. Wang, Y. Chen, R. Froehlich, J. Organomet. Chem. 689 (2004) 43.
[9] D.R. Lide, CRC Handbook of chemistry and Physics, 73rd, 6–9 (1992–1993).
[10] (a) L.J. Childs, N.W. Alcock, M.J. Hannon, Angew. Chem. Int. Ed. 40 (2001) 1079;
(b) M.J. Hannon, C.L. Painting, A. Jackson, J. Hamblin, W. Errinton, Chem. Commun. (1997) 1807.
[11] M.J. Hannon, C.L. Painting, N.W. Alcock, Chem. Commun. (1999) 2023.
[12] T. Zhang, D. Guo, S. Jie, W.-H. Sun, T. Li, X. Yang, J Polym Sci Part A: Polym Chem. 42 (2004) 4765.
[13] T. Usami, S. Takayama, Polym. J. 16 (10) (1984) 731.
[14] C. Baker, W.F. Maddams, Makromol. Chem. 177 (1976) 437.
[15] G.B. Galland, R. Quijada, R. Rojas, G.C. Bazan, Z.J.A. Komon, Maromolecules 35 (2002) 339.
[16] G.B. Galland, R.F. De Souza, R.S. Mauler, F.F. Nunes, Macromolecules 32 (1999) 1620.
[17] T. Usami, S. Takayama, Macromolecules 17 (1984) 1756.
[18] G.M. Sheldrick, SHELXTL-97, Program for the Refinement of Crystal Structures, University of Gottingen, Germany, 1997.